Technical ceramics in early iron smelting: the role of ceramics in the early first millennium BC iron production at Tell Hammeh (az-Zarqa), Jordan

H. A. VELDHUIJZEN[1]

ABSTRACT Three seasons of excavations at Tell Hammeh (az-Zarqa) in Jordan uncovered extensive remains of iron smelting and primary smithing, with production starting around 930 cal BC (AMS ^{14}C) and continuing until approximately 750 BC. The metallurgical remains consist of various types of slag, but also comprise a diversity of technical ceramics. These range from slag mixed with molten furnace wall material through vitrified furnace wall to a large quantity of tuyères. All iron production material was found in one stratigraphic context, within an area strictly used for metallurgy. The site is located in the direct vicinity of natural resources required in iron production such as water, ore, and clay. This paper explores the significant role technical ceramics play in various aspects of the Hammeh iron smelting metallurgy. Mass balance calculations on the slag, tuyères, and local ore in combination with the physical features of the tuyères show how the technical ceramics are not only tools, but form an integral part of the technology itself as well.

1. Introduction

Excavations in 1996, 1997 and 2000 at Tell Hammeh (az-Zarqa), Jordan, uncovered extensive remains of iron smelting and smithing remains, dating to approximately 1000--750 BC. Besides large quantities of various types of slag, the excavated material also consists of a diversity of technical ceramics. These ceramics range from slag mixed with molten furnace wall material through vitrified furnace wall to a large amount of tuyères. All material was found in the same stratigraphic context and within what is evidently an area strictly used for metallurgy (van der Steen, 1997, 2001, 2003; Veldhuijzen, 1998, 2000; Veldhuijzen and van der Steen, 1999, 2000). The site is located in the direct vicinity of natural resources required in iron production such as water, clay, and ore.

This paper explores the role technical ceramics play in various aspects of the Hammeh iron smelting metallurgy, not only as tools in the technological processes proper, but as an integral part of the technology itself. In that exploration, the main focus will be with the tuyères, because their particular physical features reveal the most.

2. Tuyères

A tuyère is an opening, pipe, or nozzle, through which air is supplied to a crucible, furnace, or hearth. Its primary function is to regulate and direct airflow, thereby controlling the rate of combustion. In addition, the speed and direction of the airflow may help to

increase combustion temperatures through the heightened interaction of the air blast with the fuel charge. A tuyère may also act as a barrier between the heat of the installation and the nozzle of bellows, if and when these are applied (Pleiner, 2000, p. 196). In other words, a tuyère is a variable functional part of the structure of a metallurgical installation.

Technical ceramics, i.e. ceramic materials employed for a specific technical function, are often subjected to very high temperatures, typically in excess of 1100°C, which has various effects. Most importantly, the ceramics partly vitrify and melt during the smelting or forging process. It will be argued here that in the case of Tell Hammeh, the molten technical ceramic contributes actively to the formation of the slag, thereby facilitating the production of the metal.

This direct role of technical ceramics in the metallurgical *chaîne opératoire*, which will be reflected in their outer appearance after use, allows for determination of various aspects of the metallurgical operations, such as the construction of the furnace, the method of air supply, the level of organisation, and possibly metallurgical tradition and choice. This is especially true for the tuyères, of which more than 300 individual (fragmented) specimens have been excavated at Tell Hammeh so far.

3. The clay source

Most of the Jordan Valley is covered in a Middle Pleistocene lacustrine deposit, generally referred to as the 'Lisan marls' (Maandag and Macksoud, 1969, p. 5-6; Reifenberg and Whittles, 1947). On the plateau and at the edges of the Jordan Rift Valley (Ghor), as well as in tributary valleys, including the foothills and wadi fan of the Zarqa river, these marls are in turn covered and/or mixed with calcareous fluviatile-colluvial deposits (Begin et al., 1974; Landmann et al., 2002; Maandag and Macksoud, 1969, p. 14-15, 20-21, 24; Stein et al., 1997). These 'Ghor-Lisan' soils are generally of a light and laminated nature, with a clay content that varies from approximately 10 to 20%. Occasional outcrops of marly clays occur. The soils are further characterised by a high concentration of calcium, often as calcium carbonate, varying between 25 and 50% (Maandag and Macksoud, 1969, p. 20, 25-29). Around Tell Hammeh, the soil is moderately fine textured and consists of clay loams. Nearby, a large outcrop of clay occurs, which is still used today (Maandag and Macksoud, 1969, p. 20-21). Most historical structures in the region, and on Tell Hammeh itself, are built using the clays from these soils, and the tuyères and furnace walls of the Hammeh iron production apparently form no exception. Thus, the technical ceramic is not made from a particularly refractory clay, but the locally available material.

4. The Hammeh tuyères

4.1. Shape

The Hammeh tuyères are characterised by a uniform and distinct appearance. The most distinct characteristic of the Hammeh tuyères is their square cross section of 5x5 cm. This type of tuyère is usually referred to as *block tuyères*, a shape mainly known from the La Tène and later Romano-Barbaric periods (from 450 BC onwards), concentrating in central and eastern Europe (Pleiner, 2000, p. 208-212, and Fig. 57), although these are all much bigger than the Hammeh tuyères. Almost all known tuyères in the Middle East, however,

have a circular or semi-circular ("D-shaped") cross section. The distinct square section of the Hammeh tuyères therefore may link to local or regional metallurgical tradition or technological choice (Pleiner, 2000, p. 196).

4.2. Bore

The Hammeh tuyères, in line with the European examples mentioned above, have a very small bore or air hole (Fig. 1). Throughout the length of the tuyères, it never diverges more than 2 mm from the average diameter of 10 mm, and appears to be made by insertion of, or construction of the tuyère around, a straight stick or reed. The narrowness of the air hole indicates that the tuyères were constructed for use with bellows, since a natural draught furnace would require far wider air inlets (i.e. > 20 mm diameter). At the rear end, the bore has been widened, apparently with a finger, to a depth of 45 mm (two digits) and a diameter of 30 mm. At the same time, this leads to a larger tuyère cross section of around 8x6 cm, with most tuyères being predominantly widened to the lateral sides. It is assumed that this widened bore accommodated the nozzle of the bellows.

4.3. Angle

The narrow borehole makes the tuyères very susceptible to blocking by slag and molten ceramic. To resolve this, tuyères are often placed with their nozzle slightly sloping down. This seems to be the case at Hammeh as well, since a reducingly fired zone at the tuyère nozzles, marking the part that protruded through the furnace wall into the furnace chamber, indicates a downward inclination of around 20°. This angle is further confirmed by the sloping face of most vitrified nozzles (see Fig. 1).

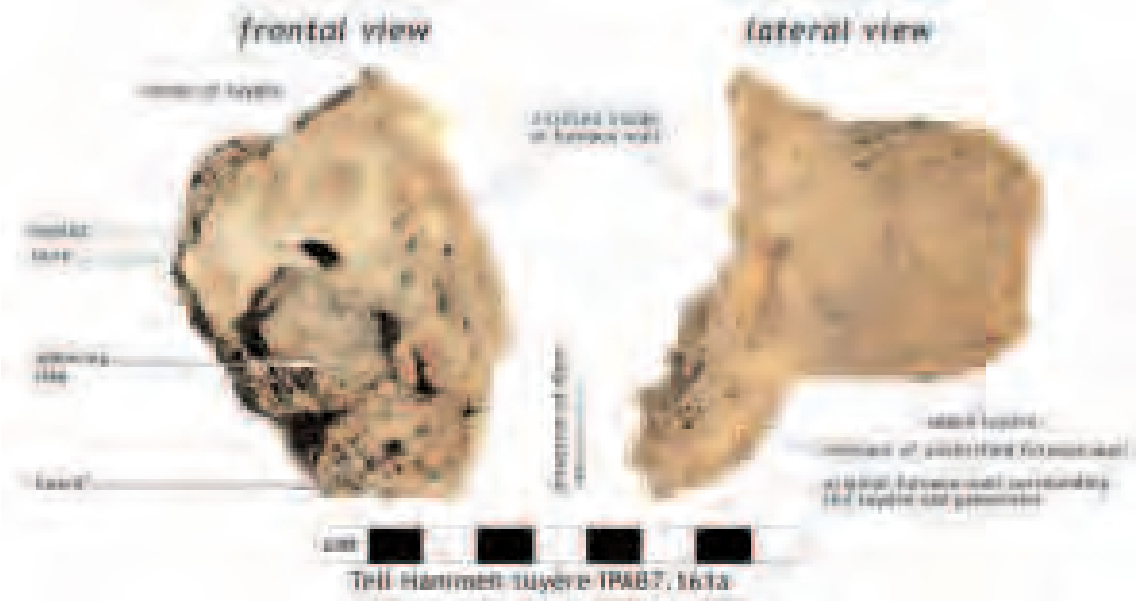

FIG. 1 – Frontal and lateral view of vitrified nozzles.

4.4. Length

Four of the tuyères excavated so far seem to be 'complete', meaning that they range from a rear end with widened bore (where the bellow was inserted), to a vitrified nozzle (where the tuyère was exposed to severe heat inside the furnace, see Fig. 1). No definite conclusions can be drawn about the original full length of the tuyères, but these four 'complete' tuyères all measure around 35 cm. Among the material, a few very small nozzles, 3 x 3 cm in section and mostly unvitrified, are present. This may hint at a longer total shape, with a tapering front.

4.5. Standardisation

Another important feature is the quantity of tuyères, and their standardisation in shape and size. Hardly any variation of size seems to occur, except for some possible tapering of the shape towards the nozzle, the widening of the bore at the outside end, and some possible shrinkage and expansion effects due to the heat exposure during use. There are no indications for the use of a mould of any kind. The high degree of uniformity within the large quantity of tuyères seems to point to regular or even mass production, as opposed to just an 'experimental stage' of metallurgy. The degree of standardisation of tuyère production may well be related to concepts of efficiency (Costin, 2001, p. 289-291) and control and organisation (Costin, 2001, p. 301-303) of the smelting operations at Hammeh.

4.6. Vitrification and melting of the ceramic

The molten and vitrified tuyère nozzles clearly show the results of liquefied ceramic, and are often in direct contact with slag. Just above the bore, the vitrified ceramic often forms a slightly protruding and overhanging 'eyelid', where ceramic and/or slag material flowing down was pushed up and forward by the air blast. Similarly, one side of the tuyères often shows a (often small, usually broken off) extension or 'beard' of vitrified ceramic and/or slag beyond the tuyère proper. Both features helps to identify which side of the tuyère was top or bottom. Additionally, the fact that some tuyère fragments show remains of furnace wall attached to them, clearly shows that some form of shaft must have been present in the Hammeh process. Most of the vitrification effects described here can be observed in Fig. 1.

5. Contribution of technical ceramics to the slag formation

5.1. Formation of slag

'Regular' bloomery slag is characterised by predominantly fayalite (i.e. Fe_2SiO_4) in a glassy matrix, with varying amounts of free iron oxide in the form of wüstite. The total percentage of FeO usually ranges between 60 and 70%. Bulk chemical analysis of the tapped smelting slag from Hammeh by (P)ED-XRF, however, shows a relatively low FeO (ca. 50%) and high CaO (up to 20%) content. This is consistent with the relatively low grade of fayalite formation visible in these samples.

If less FeO ends up in the slag, more FeO must have been reduced to metallic iron, i.e. a low FeO percentage in slag indicates that a higher yield of metallic iron was achieved in the smelting process. During the formation of slag, iron oxide may be substituted by calcium oxide, enhancing the formation of pyroxenes (i.e. $(Fe,Ca)_2Si_2O_6$) and glass rather than fayalite. In addition, Ca^{2+} can replace part of the Fe^{2+} in olivines such as fayalite; similarly Mg^{2+} and Mn^{2+} can replace part of Fe^{2+} in both spinels and olivines. This frees additional iron oxide for reduction to metallic iron (Serneels, 1993, p. 29-31). Both fuel ash (Crew, 2000) and the melting technical ceramics may contribute towards this, beyond the original presence of calcium, magnesium or manganese in the ore that is used (Serneels and Crew, 1997).

An active contribution of molten ceramic to the fluxing and formation of slag has been assumed previously, primarily with the (ethnographically observed) vertical tuyère smelting operation of the *Mafa* in Cameroon (David et al., 1989). However, little archaeometric data is available on this subject, besides the pioneering research on the contribution of technical ceramics and fuel ash to the formation of slag, and the role this contribution may play in enhancing the process, by Vincent Serneels and Peter Crew (Crew, 2000, on clay-fuel ash-slag relations; Serneels and Crew, 1997, on ore-slag relations).

5.2. Comparison of Warda ore and Hammeh slag

Mass balance calculation, using the compositions of a sample from the local Mugharet al-Warda ore-site, HA97 65 (Veldhuijzen, 1998), and a typical tapped smelting slag from Hammeh, HA2002 A7, allows the determination of a hypothetical slag, i.e. the slag that would result from smelting this particular ore if there are no other contributions to the process. It should be noted that all other possible influences in slag formation, such as redox conditions and the contribution and behaviour of fuel ash, are ignored here, that the haematite ore is presented as FeO, and that the single samples are treated as roughly representative of all ore, slag and ceramic material. The calculations here should therefore be considered only as a first step into the investigation of the ceramic contribution to Hammeh slag formation.

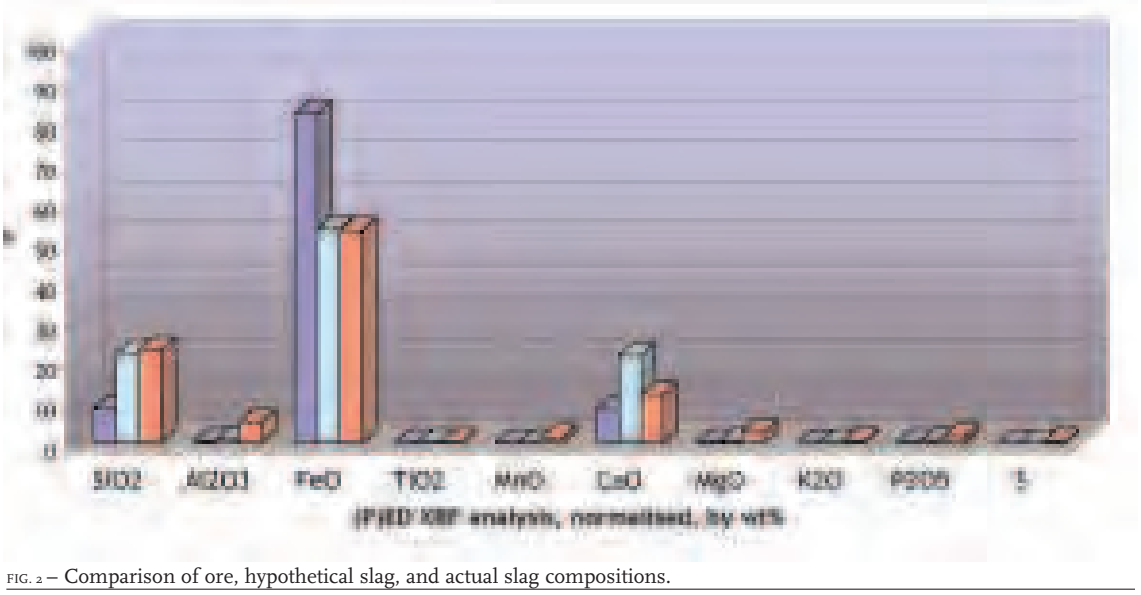

FIG. 2 – Comparison of ore, hypothetical slag, and actual slag compositions.

When aiming to produce a hypothetical slag with the same iron oxide content as the actual slag, 100 kg of Warda ore would yield about 48 kg of metallic iron, and result in some 38 kg of slag with approximately 53% FeO. Fig. 2, however, clearly shows that such a hypothetical slag does not match the actual Hammeh slag at all when the remaining concentrations of Al_2O_3, TiO_2, MnO, CaO, MgO, K_2O and P_2O_5 are concerned. It therefore follows that the Warda ore on its own can not produce the slag found at Tell Hammeh.

5.3. Contribution of technical ceramic to Hammeh slag formation

It is only when we consider a possible contribution of technical ceramics to the slag formation at Hammeh that we can adjust this imbalance. Fig. 3 shows how the addition of 21 kg of technical ceramic (a sample of the local Lisan clay, HAC1) leads to a hypothetical slag that closely resembles the actual Hammeh slag, with the exception of MnO, MgO and P_2O_5. These, however, are typical fuel ash elements, and likely stem from there, as demonstrated by Serneels and Crew (Crew, 2000; Serneels and Crew, 1997). With the additional ceramic material, the Hammeh smelting process would roughly yield 33 kg of metallic iron for each 100 kg of Warda ore, and leave 79 kg of slag.

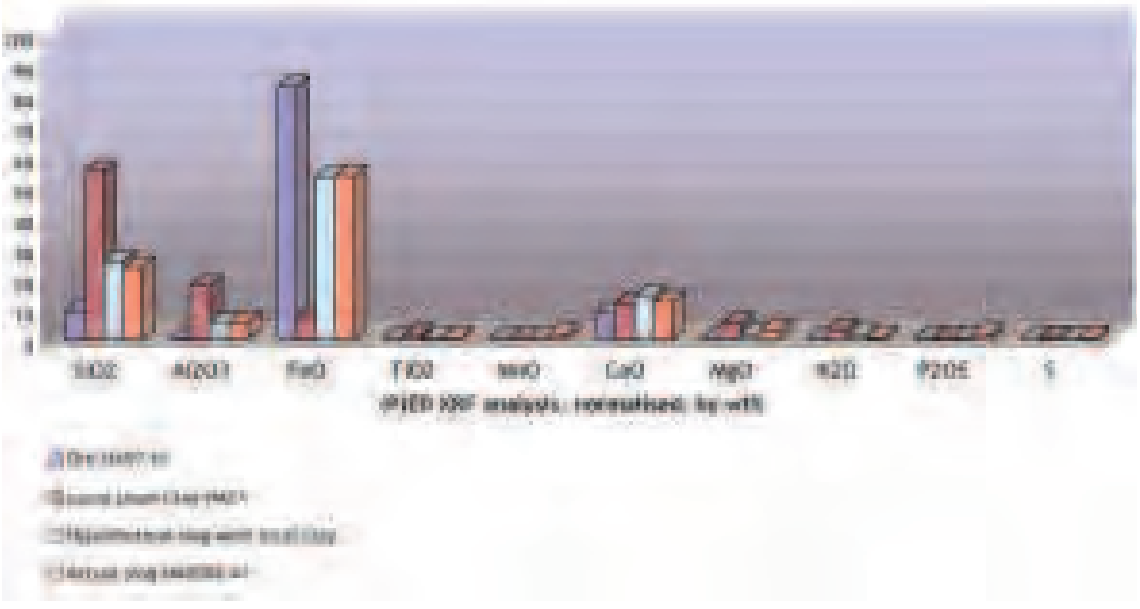

FIG. 3 – Comparison of ore, clay, hypothetical slag with ceramic contribution, and actual slag compositions.

6. Conclusions

From the above it is clear that technical ceramics play a large and crucial role in the iron smelting operations on Tell Hammeh (az-Zarqa). From the physical appearance of the tuyères alone, it can be concluded that a shaft furnace as well as bellows were used. The high number and standardised size and shape of the tuyères point at smelting operations at Hammeh that are well beyond experimental stages of production. At the same time, the typical square section of the tuyères may tie in with local or regional metallurgical traditions or technological choice.

The physical appearance of the tuyères, with their heavily molten and vitrified nozzles, strongly supports the chemical data that indicate an important contribution of technical

ceramics to the formation of the Hammeh slag. From the combination of these physical and chemical data, it can be concluded that the Hammeh smelters purposefully applied sacrificial tuyères to facilitate the production of iron.

7. Acknowledgements

The development of the calibration method described here is part of ongoing PhD research, carried out at the Wolfson Archaeological Science Laboratory, Institute of Archaeology, UCL, under the supervision of Professors Thilo Rehren and Vincent Pigott. It is sponsored by BHP Billiton through the Institute for Archaeo-Metallurgical Studies (IAMS).

The excavations at Tell Hammeh (az-Zarqa) are part of the *Deir ᶜAlla Regional Project*, a joint undertaking of Leiden University (the Netherlands) and Yarmouk University (Jordan) in conjunction with the Department of Antiquities of Jordan. I am indebted to its Scientific Directors, Zeidan Kafafi (YU) and Gerrit van der Kooij (LU), for their support, allowing me to direct the excavations at Hammeh in 2000 with scientific excavation of the iron production remains as main aim, and enabling me to select freely from all excavated material. I am also grateful to the Department of Antiquities of Jordan, for their kind permission to take this material to the UK for further study.

NOTES

[1] Institute of Archaeology, University College London.

REFERENCES

BEGIN, Z. B.; ERLICH, A.; NATHAN, Y. (1974) - Lake Lisan – The Pleistocene precursor of the Dead Sea. *Geological Survey of Israel Bulletin*. Jerusalem. 63, p. 1-30.

COSTIN, C.L. (2001) - Craft production systems. In FEINMAN, G. M.; PRICE, T. D., eds. - *Archaeology at the Millennium: a sourcebook*. New York: Kluwer Academic/Plenum Publishers, p. 273-327.

CREW, P. (2000) - The influence of clay and charcoal ash on bloomery slags. In CUCINI TIZZONI C., TIZZONI M., eds. - *Il ferro nelle alpi. Giacimenti, miniere e metallurgia dall' antichità al XVI secolo. Atti del convegno/Iron in the alps. Deposits, mines and metallurgy from antiquity to the XVI century. Proceedings of the conference, Bienno, ottobre 1998*. Breno: Commune di Bienno, p. 38-48.

CREW, P.; CREW, S., eds. - *Early Ironworking in Europe. Archaeology and Experiment. Abstracts of the International Conference at Plas Tan y Bwlch 19-25 Sept. 1997*. Maentwrog: Plas Tan y Bwlch Occasional Papers No 3.

CUCINI TIZZONI C., TIZZONI M., eds. - *Il ferro nelle alpi. Giacimenti, miniere e metallurgia dall' antichità al XVI secolo. Atti del convegno/Iron in the alps. Deposits, mines and metallurgy from antiquity to the XVI century. Proceedings of the conference, Bienno, ottobre 1998*. Breno: Commune di Bienno.

DAVID, N.; HEIMANN, R.; KILLICK, D.; WAYMAN, M. (1989) - Between bloomery and blast furnace: Mafa iron-smelting technology in North Cameroon. *The African Archaeological Review*. Houston, TX. 7, p. 183-208.

LANDMANN, G.; ABU QUDAIRA, G. M.; SHAWABKEH, K.; WREDE, V.; KEMPE, S. (2002) - Geochemistry of the Lisan and Damya Formation in Jordan, and implications for paleoclimate. *Quaternary International*. Amsterdam. 89:1, p. 45-57.

MAANDAG, F. L. A.; MACKSOUD, S. W. (1969) - *Annex C: Soils and Drainage. Jordan Valley Project: Agro- and Socio-Economic Study, final report. II*. Amman, Jordan: The Hashemite Kingdom of Jordan - Jordan River and Tributaries Regional Corporation//Dar al-Handasah Consulting Engineers//Netherlands Engineering Consultants (NEDECO), p. 1-43.

PLEINER, R. (2000) - *Iron in Archaeology. The European bloomery smelters*. Praha: Archeologick_ Ústav Av Cr.

REIFENBERG, A.; WHITTLES, C. A. (1947) - *The soils of Palestine*. London: Thomas Murby Co.

SERNEELS, V. (1993) - *Archéométrie des scories de fer, recherches sur la sidérurgie ancienne en Suisse occidentale*. Lausanne: Cercle Vaudois d'Archéologie Préhistorique et Historique (CVA) (Cahiers d'Archéologie Romande; 61).

SERNEELS, V.; CREW, P. (1997) - Ore-slag relationships from experimentally smelted bog-iron ore. In CREW, P.; CREW, S., eds. - *Early Ironworking in Europe. Archaeology and Experiment. Abstracts of the International Conference at Plas Tan y Bwlch 19-25 Sept. 1997*. Maentwrog: Plas Tan y Bwlch Occasional Papers No 3, p. 78-82.

STEIN, M.; STARINSKY, A.; KATZ, A.; GOLDSTEIN, S. L.; MACHLUS, M.; SCHRAMM, A. (1997) - Strontium isotopic, chemical, and sedimentological evidence for the evolution of lake Lisan and the Dead Sea. *Geochimica et Cosmochimica Acta*. Amsterdam. 61, p. 3975-3992.

VAN DER STEEN, E. J. (1997) - Excavations at Tell el-Hammeh. *Occident & Orient*. Amman. 3, p. 12-14.

VAN DER STEEN, E. J. (2001) - Excavations at Tell el-Hammeh. In *Studies in the History and Archaeology of Jordan VII*. Amman: Jordan Press Foundation p. 229-232.

VAN DER STEEN, E. J. (2003) - *Tribes and Territories in Transition: the central East Jordan Valley and surrounding regions in the Late Bronze and Early Iron Ages: a study of the sources*. Groningen: Rijksuniversiteit Groningen.

VELDHUIJZEN, H. A. (1998) - *Early iron smelting. Analysis and interpretation of Late Iron Age Iron smelting remains from Tell Hammeh az-Zarqa, Jordan*. Leiden: Leiden University, Faculty of Archaeology, unpublished M.A. Thesis.

VELDHUIJZEN, H. A. (2000) - Early Iron Production found in the Jordan Valley. *Orient Express*. 1, p. 9-12.

VELDHUIJZEN, H. A. (2003) - *'Slag_Fun' - A New Tool for Archaeometallurgy: Development of an Analytical (P)ED-XRF Method for Iron-Rich Materials*. London: University College, Institute of Archaeology (Papers from the Institute of Archaeology; 14), p. 102-118.

VELDHUIJZEN, H. A.; VAN DER STEEN, E. J. (1999) - Iron Production Center Found in the Jordan Valley. Near Eastern Archaeology 62 (3), p. 195-199.

VELDHUIJZEN, H. A.; VAN DER STEEN, E. J. (2000) - Early iron smelting (Tell-Hammeh, Jordan). *Archaeology*. Boston. 53:1, p. 21.

Developing the linear modulated OSL (LM - OSL) as a new tool for ceramic dating

A. ZINK[1] J. CASTAING[1]

ABSTRACT Optically stimulated luminescence (OSL) is used, as well as thermoluminescence (TL), in our laboratory to investigate the authenticity of ceramic art objects from museum collections. A great advantage of the OSL is to need only a few samples using a single aliquot regeneration (SAR) technique to obtain ages with a good accuracy. On the other hand, the OSL intensity integrates the signal from various traps: some of them may be unstable. Hence a detailed investigation is needed for all new objects. The linear modulated - optically stimulated luminescence (LM-OSL) technique could be a good alternative. The regular increase of the stimulation power permits to monitor the various traps in the crystal. The advantage of the LM-OSL is to work with low heat (125°C) reducing the risk of thermal perturbation of the crystal usually encountered with TL. Various bricks and sands are investigated. The choice of the best stimulation power depending on the type of ceramic is discussed. An example of direct dating using SAR-LM-OSL is presented and compared to TL dating obtained on the same sample.

1. Introduction

Thermoluminescence (TL) is widely used to date ceramics and terracotta since the 1970's (Aitken, 1985). As the other dating methods, TL is based on two properties of the material. It is a physical process which evolves with time and there is an initial instant (Giot and Langouët, 1984). The physical process is the accumulation of absorbed energy coming from the ambient radioactivity into the minerals. We assume that the content in radioelements (uranium, thorium and potassium) is constant and then the dose received during one year, the annual dose, is constant. The initial instant is a heat at above 500-700°C which resets to zero the anterior accumulated dose. During the TL measurement, a new heat treatment is conducted. During the heat, the previous accumulated dose, known as palaeodose, is released under light emission, the so-called "natural TL". To calibrate the emission, it is necessary to re-irradiate the sample with an artificial radioactive source before to measure again the signal. But during the first heating in laboratory, some changes in the mineralogy can occur in the sample, such as the diffusion of impurities or the phase transition from α quartz to β quartz. Then, the sample used for the calibration is, from a mineralogical point of view, not strictly the same as in the initial conditions. To avoid this problem, a particular protocol, known as additive TL (Aitken, 1985), is employed using various aliquots, some for recording the natural TL and the others to measure a mixed natural + laboratory induced TL. It is time- and material-consuming.

In the mid of 1980's, a new dating method, the optical stimulated luminescence (OSL), was developed using light (visible or near IR) to stimulate the emission, instead of the heat. Being optical stimulation an energy soft process, there is no perturbation of the

sample; then, it is possible to work with a single aliquot (Murray and Wintle, 2000). The OSL technique is then a good alternative to TL when the size of the sample is strongly limited as it is, generally, for ceramics from museums.

The usual OSL technique, or continuous wave OSL (CW-OSL), is an integrating method. Under stimulating light, all the signal is received in a short time and it is not possible to discriminate between the various kinds of emission. Only the stable signals (i.e. with lifetimes much greater than the archaeological age) are used to date and there is no straightforward way to identify them in CW-OSL. In TL, each signal is identified by a peak in the glow curve. The best temperature range is defined by the so-called 'plateau' test (Aitken, 1985). Bulur (1996) developed a technique, the linear modulated OSL (LM-OSL), in which the power of the stimulation light increases from zero to a maximum during the measurement. With this technique, it is possible to discriminate the various signals of the OSL. In this paper, known materials are investigated by LM-OSL to assess the ability of this technique to improve dating of museum objects.

2. Experimental details

2.1. Sample preparation and the number of aliquots

Sample preparation was similar to the routine procedure followed for dating. The sands and powders were crushed in an agate mortar. The tiles were sampled using a minidrill with 1,8 mm tungsten carbide bit. After etching by HCl and washing by water, ethanol and acetone, the 4-10 µm fraction is selected by sedimentation into 8 cm height acetone and deposited on 9,8 mm diameter discs. All these operations, but the HCl etching, are automated (Zink et al., 2002).

For the routine procedure to date museum objects, the sample is limited to 100 mg and the corresponding fine grain fraction is not enough to be split in more than twenty aliquots (or discs). Thirteen are used for additive TL measurements (Fleming, 1979), four for OSL, one for test. The last two are conserved for some possible further tests.

The main aim of the study was to see if LM-OSL measurements can be usefully incorporated in this procedure without increasing the number of aliquots. For that purpose, various kinds of materials were used, such as terracotta, as shards or powders, and sands. The powders were annealed at 500°C during several hours to eliminate all previous TL/OSL signals, before irradiation with β or X-ray source. For X-ray stimulation, 420/10 SEIFERT isovolt X-ray tubes (Beryllium windows) were used with the sample located at 1.3 m from the tube. The β source $^{90}Sr/^{90}Y$, incorporated into the measurement apparatus, provided a dose rate of 0.13 Gy/s (at the date of 1.06.2003).

2.2. Measurement apparatus

The measurements were performed with a Risø TL/OSL DA-15 reader. The luminescence was recorded using a photomultiplier tube EMI 9235 QA with 7,5 mm Hoya U340 filter. The blue light stimulation was provided by 18 pairs of blue diode (470 nm) delivering a maximum irradiance of 19 mW cm^{-2} at the sample position. Infrared stimulation used an IR laser diode at 830 nm with a maximum irradiance of 450 mW cm^{-2} at the sample. To limit the effects of cross-irradiation and cross-bleaching (Bray et al., 2002), the discs were put only on the odd positions. All measurements were recorded by integrating one second per channel.

2.3. *Experiments*

A basic LM-OSL experimental sequence is described in table 1. It was adapted from a classical double-OSL measurement (Murray and Wintle, 2000).

TABLE 1

The double SAR CW-OSL procedure and the version adapted to LM-OSL.

	Basic double SAR CW-OSL	intensity observed	Adapted to LM-OSL	Intensity observed
1	Give dose Di	—	Give dose Di	—
2	ph 200°C 0s	—	ph 200°C 0s	—
3	IR-OSL 100s at 60°C	—	IR-OSL 200s at 60°C	—
4	BL-OSL 100s at 125 °C	Li	LM-OSL 0-100% 200s at 125 °C	Li
5	Give test dose Dt	—	BL-OSL 200s at 125 °C	—
6	ph 200°C 0s	—	LM-OSL 0-100% 200s at 125 °C	Lo
7	IR-OSL 100s at 60°C	—	Give test dose Dt	—
8	BL-OSL 100s at 125 °C	Ti	ph 200°C 0s	—
9	return to 1		IR-OSL 200s at 60°C	—
10			LM-OSL 0-100% 200s at 125 °C	Ti
11			BL-OSL 200s at 125°C	—
12			LM-OSL 0-100% 200s at 125 °C	To
13			return to 1	

The normalized response to a dose Di (i={0,1,2,3}) is Li/Ti for the basic double SAR and (Li-Lo)/(Ti-To) for the LM-OSL double SAR.

In a first step, a dose D_0 was given to the sample. It could be a natural irradiation due to environment after the last heat, the so-called palaeodose, or an artificial irradiation made with a calibrated source in the laboratory (line 1 in table 1). The feldspar contribution was removed during the infrared stimulation (IR-OSL). The LM-OSL was recorded under blue stimulation with a power rate of 0.095 mW cm^{-2} s^{-1} (the maximum power being reached in 200s). After the LM-OSL, the sample was stimulated during 200s with the diodes at full power to eliminate all luminescence (line 5 in table 1). Then, a second LM-OSL recorded the background. To normalise the sensitivity, the cycle was repeated with a test dose (1.3 Gy). To calibrate an unknown dose D_0, we followed a single aliquot regeneration (SAR) process. Three different regenerating doses D_i (i={1,2,3}) were employed which interpolated D_0. A measurement without dose gives the recuperation value, normally close to zero. The calibrations were concluded with a second measurement of D_1 to test the recycling (1.00±0.15 is an acceptable value). In total, the sequence displayed in table 1 was repeated six times on the same aliquot to determine the unknown dose D_0.

2.4. *LM-OSL curve deconvolutions*

For a single trap of first order, Bulur (1996) described the LM-OSL curve as a function of time t by the following equation:

$$L(t) = -\frac{dn}{dt} = n_0 \frac{\sigma I_0}{\theta} t \exp\left(\frac{\sigma I_0}{2\theta} t^2\right)$$

n_o is the initial trapped charge number related to the trapping probability, _ is the cross section (cm^2) related to the detrapping probability, I_o is the maximum stimulation intensity ($I_o = P/h\upsilon$ where P is the maximum irradiance — $W\ cm^{-2}$ — and $h\upsilon$ the photon energy - eV) and θ is the total measurement time (s). The product $b = \sigma I_o$ is the frequency of optical detrapping (Hz).

For a usual sample, the LM-OSL curve is the addition of the signal from several traps. Each trap is defined by σ and n_o. To estimate σ and n_o, the experimental curves were fitted by the addition of several Bulur's equations. The curves were simulated using 1 to 5 components, the parameters being adjusted for each sample. The best fit was obtained by minimising the χ^2-value ($\chi^2 = \sum_t (L_{obs}(t) - L_{fit}(t))^2$ using the SOLVER macro in an EXCEL spreadsheet.

3. Results

3.1. Properties of polymineral LM-OSL

The LM-OSL curves for various bricks and sands irradiated 47 Gy and read with a power rate of 0.095 $mW\ cm^{-2}\ s^{-1}$ are plotted in Fig 1. Cluny B and CMB are terracotta, that is, mixtures of different minerals; it is not surprising that three peaks were found through the analysis. For sands which are dominated by quartz, the LM-OSL curve displayed almost only one peak. The corresponding parameters of the components are summarised in table 2. Similar value of σ can be noticed, especially between CMB and Sand A. The reference values in literature are very limited. Only pure quartz was actually investigated by LM-OSL under blue light stimulation (Jain et al., 2003; Singarayer and Bailey, 2003; Tsukamoto et al., 2003). Jain et al. (2003) identified seven components, called respectively ultra-fast, fast, medium, slow1, slow2, slow3 and slow4. Singarayer and Bailey found the same value of σ, but the ultra-fast and the slow1 components were not identified. The values founded by Tsukamoto et al. who made the distinction between tephric and volcanic quartz are different from the other authors who seem to work on sedimentary quartz. Our results seemed more consistent with those from Tsukamoto et al (2003). Hence, Cluny B was more consistent with tephric quartz, while CMB and sand A could be volcanic quartz. Sand B seemed a mixing of volcanic and tephric quartz.

TABLE 2

The cross section (σ) and the number of initial trapped electrons (n) of the components fitted to LM-OSL curves plotted on Fig. 1.

	σ1 (cm^2)	n1	σ2 (cm^2)	n2	σ3 (cm^2)	n3
Cluny B	$7.1\ 10^{-18}$	$1.5\ 10^5$	$2.5\ 10^{-18}$	$1.1\ 10^5$	$5.9\ 10^{-19}$	$7.2\ 10^4$
CMB	$1.2\ 10^{-17}$	$5.2\ 10^3$	$1.8\ 10^{-18}$	$1.6\ 10^4$	$2.2\ 10^{-19}$	$5.0\ 10^4$
Sand A	$1.1\ 10^{-17}$	$1.3\ 10^6$	$1.8\ 10^{-18}$	$1.0\ 10^5$		
Sand B	$1.5\ 10^{-17}$	$9.9\ 10^3$	$6.6\ 10^{-19}$	$2.3\ 10^3$		

(power rate:0.095 $mW.cm^{-2}.s^{-1}$; Cluny B: Roman brick 2nd century AD; CMB: a modern brick; and Sand A and Sand B: two commercial sands)

FIG. 1 – LM-OSL curves for various bricks and sands (a - Cluny B Roman brick II century AD; b- CMB modern brick 19th century AD; c-Sand A; d-Sand B). The LM-OSL component fitted and their sum are also plotted. (irradiation 47 Gy; power rate 0.095 mW cm^{-2} s^{-1})

3.2. *Effect of the power rate*

By increase of the total duration of the stimulation from 200 to 6000 s, we decrease the power rate from 0.095 mW cm^{-2} s^{-1} to 0.0032 mW cm^{-2} s^{-1}. The measurements were made on two samples (Cluny and CMB). The values of σ were fixed for each sample to the values found for a stimulation during 200s (see above). With such an initial condition, the fit was globally satisfying. At low power rate, one to two new traps were added to optimise the fit, corresponding to traps with lower cross sections. We observed a relative stability of the charge trapped concentration.

3.3. *Thermal stability*

The effect of the preheat temperature was investigated for Cluny and CMB. After irradiation to a fixed dose, the sample was preheated to a temperature T between 180°C and 400°C at 20°C steps. On Fig. 2, the change of intensity of the various components are shown with a normalisation to the preheat at 180°C.

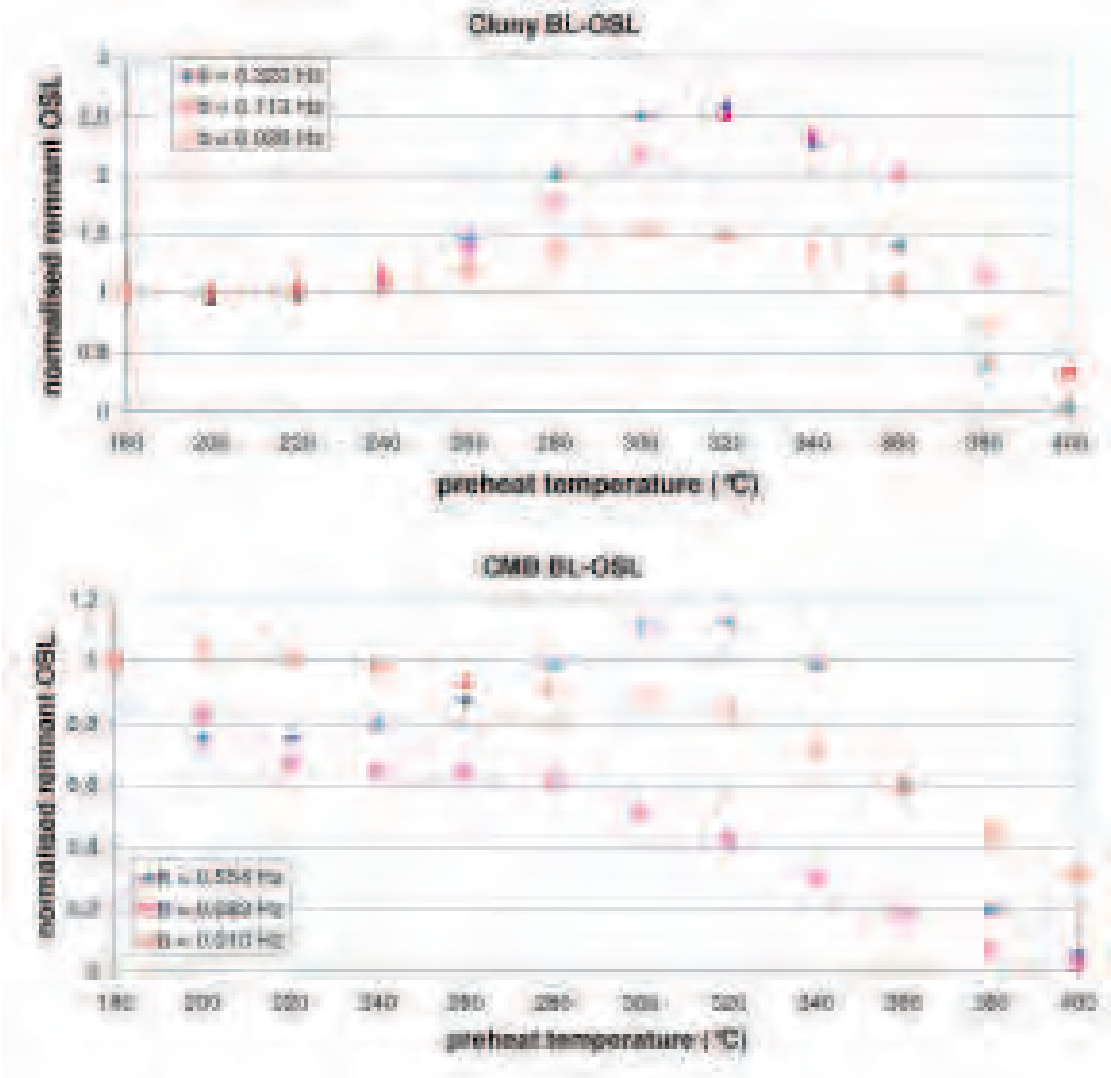

FIG. 2 – Change of intensity of the various components of the LM-OSL with the preheat temperature for a Roman brick – Cluny B and a modern brick – CMB (normalization to the preheat at 180°C)

For Cluny, the three components have the same evolution. The signals were stable until around 250°C. Then we observed a high sensitisation from 260 to 320°C, followed by a decrease. At 400°C, the component 1 is negligible, when the component 2 and 3 were reduced to around 30% of the signal for preheat at 180°C.

The evolution for CMB is more complex and the signal is less stable. The first component ($\sigma = 1.2\ 10^{-17}$ cm^2) has an evolution similar to the components Cluny, with a strong sensitisation around 300-320°C. The second component ($\sigma = 1.8\ 10^{-18}$ cm^2) shows two successive decays, the first below 220°C, the second above 280°C. The last component ($\sigma = 2.2\ 10^{-19}$ cm^2) was stable until 240°C before decreasing.

3.4. Direct dating using LM-OSL

Singarayer and Bailey (2003) suggested to use the slower component from quartz (Slow4 following the nomenclature of Jain et al., 2003) to date all geological samples (>>100 ka). They used a SAR protocol and resolved the components of the LM-OSL curves. Such a process could be useful for old samples (the cited sample gives a palaeodose of '696±438 Gy') with a strong intensity of the luminescence. Choi et al. (2003) used indirectly the LM-OSL measurement to separate the components within the CW-OSL curve in the aim of dating. For samples with a low natural emission such as archaeological ceramics (usually 1-10 Gy), it is not possible to obtain a valuable fit, and then to separate the components. The precision on the fit is limited by the signal/noise ratio of the measurement (Fig. 3). Hence, for such a sample we suggest to use another method for which the fit is not needed.

We decided to process the LM-OSL data as for TL with the so-called 'plateau' test. After the measurement of the sample by a SAR protocol, as described above (table 1), a dose response curve was plotted for each channel (i.e. each second of illumination). Then, the palaeodose De was reported as a function of the illumination power. Analogue to the TL, we searched the power range where De is maximal and constant. We assume that for such a range, the dominant component is stable (i.e. its lifetime is much greater than the archaeological age).

We tried this method first to estimate the dose from X ray irradiated materials in the framework of a study on the effects of radiography on TL measurements (Castaing et al. submitted). Six tiles and sands were previously annealed to 550°C during few hours, and then irradiated with the X-ray source used in our laboratory for the object radiographies. The irradiation was made under 400 kV 4 mA during 90 minutes. The results (Table 3) were in agreement with the CW-OSL results.

TABLE 3

The equivalent in seconds of beta irradiation measured by linear modulated-OSL (LM-OSL) and continuous wave-OSL (CW-OSL) of an X-ray irradiation of 400 kV, 4mA during 90 minutes.

Specimen #	LM-OSL	CW-OSL	Specimen #	LM-OSL	CW-OSL
CMB-P		421 ± 50	Meggido P	339 ± 17	413 ± 21
CMB shard	338 ± 47		Sand A	286 ± 48	257 ± 10
XIX P	305 ± 21	354 ± 10	Sand B	258 ± 55	284 ± 11
Cluny P	340 ± 19	284 ± 4	Sand MNgg		276 ± 7
Average	311 ± 10	327 ± 3			

An archaeological brick from St Denis (France) was dated previously by TL and OSL in the framework of an intercalibration program between the C2RMF and the ITN, Sacavém, Portugal (Richter et al., 2003). For each methods (TL and OSL), the results (table 4) were similar for the two laboratories. But a small underestimation of the OSL compared to the TL was observed. We decided to date the brick using the LM-OSL SAR protocol (Fig. 3) with two different preheat (200 and 250°C). The signal was very low. A plateau was present between 5 and 20% power levels. Integrating the signal between 5 and 20% corresponding to the peak, we obtained an equivalent dose of 2,2±0,3 Gy in close agreement with the CW-OSL measurements.

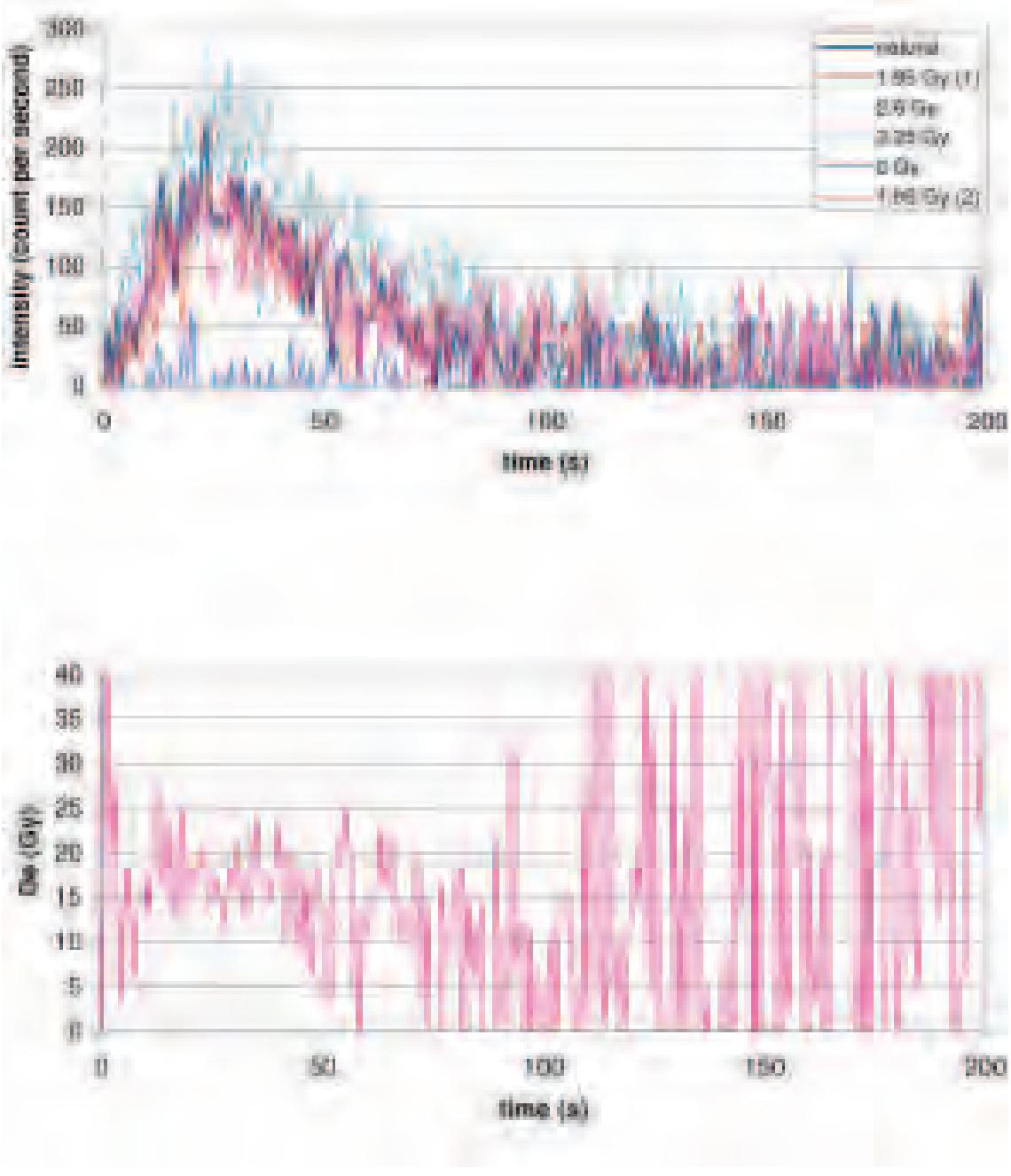

FIG. 3 – Single aliquot regeneration protocol applied to the LM-OSL signal of a medieval brick (St Denis 57a). Top curves: LM-OSL curves. Bottom curve: the equivalent dose (De) as function of the irradiation time, the so-called 'plateau test'.

TABLE 4

Equivalent dose (in Gy) for a medieval brick from St Denis (France, 13th century) by various methods and dating techniques at the C2RMF (Paris) and at the ITN (Sacavém). The LM-OSL results are presented and commented in the present paper.

LM-OSL plateau	LM-OSL $\sigma 1^{*}$	LM-OSL $\sigma 2^{*}$	LM-OSL $\sigma 3^{*}$	CW-OSL C2RMF	CW-OSL ITN	TL** C2RMF	TL** ITN
2.2±0.3	2.1±0.3	2.3±0.3	0.4±0.4	2.2±0.3	2.39	2.6±0.3	2.70±0.08

* Component 1: $\sigma 1 = 9.2\ 10^{-18}\ cm^{-2}$
Component 2: $\sigma 2 = 2.9\ 10^{-18}\ cm^{-2}$
Component 3: $\sigma 3 = 4.4\ 10^{-19}\ cm^{-2}$

** For the discussion on the TL results see Richter et al. (2003).

We applied also a component-resolved method (see section 2.4). The parameters for the St Denis brick were based on LM-OSL measurements of coarse grains irradiated with 31 Gy after bleaching 5 minutes under blue light. Three components were identified. The first two components corresponded to the main peak and agreed together (Table 4). On the other hand the slow component 3, responsible of emissions at high power radiance, showed a very low value of the equivalent dose 0,4 ± 0,4 Gy. It is not surprising that the plateau range excluded the slow component. Due to its low intensity, the component 3 did not yield to a large underestimation of the CW-OSL dating which integrates the three components. It explains the good agreement between LM-OSL and CW-OSL dating.

4. Conclusions

LM-OSL is a simple experimental approach to detect the presence of various traps. Varying the measurement conditions gives the possibility of choosing the best signal for the purpose of dating. Our LM-OSL measurements showed that the CW-OSL signal from polymineral fractions extracted from ceramics or sands can not be easily reduced to quartz signals. Hence a LM-OSL study is useful for all new samples before dating measurements. Moreover the LM-OSL can be used directly to date. For such a purpose, a simple plateau method can be used, giving results in agreement with the more complex component-resolved method. The plateau method is particularly useful for ceramic dating where the luminescence signal is low.

Acknowledgements

Our special thank to J.-R. Gaborit for providing samples.

We want to thank E. Porto for sampling and preparation and T. Borel for X-ray irradiation.

The intercalibration with the luminescence dating unit in Sacavém, as well the funding of the participation to the EMAC03 are part of a bilateral protocol ICCTI/French Embassy n.° A0521.

NOTES

[1] Centre de Recherche et Restauration des Musées de France, UMR 171 - CNRS - MCC, 6 rue des Pyramides, 75 041 Paris Cedex 01, France.

REFERENCES

AITKEN, M. J. (1985) - *Thermoluminescence Dating*. London: Academic Press.

BRAY, H. E.; BAILEY, R. M.; STOKES, S. (2002) - Quantification of cross-irradiation and cross-illumination using a Risø TL/OSL DA-15 reader. *Radiation Measurement*. Amsterdam. 35, p. 275-280.

BULUR, E. (1996) - An alternative technique for optically stimulated luminescence (OSL) experiment. *Radiation Measurements*. Amsterdam. 26, p. 701-709.

CHOI, J. H.; MURRAY, A. S.; CHEONG, C. S.; HONG, D. G.; CHANG, H. W. (2003) -The resolution of stratigraphic inconsistency in the luminescence age of marine terrace sediments from Korea. *Quaternary Science Review*s. Amsterdam. 22, p. 1201-1206.

GIOT, P.-R.; LANGOUËT, L. (1984) - *La datation du passé: la mesure du temps en archéologie*. Rennes: Groupe des Méthodes Physiques et Chimiques en Archéologie.

JAIN, M.; MURRAY, A. S.; BOETTER-JENSEN, L. (2003) - Characterisation of blue light stimulated luminescence components in different quartz samples: implications for dose measurement. *Radiation Measurements*. Amsterdam. 37, p. 441-449

MURRAY, A. S.; WINTLE, A. G. (2000) - Luminescence dating of quartz using an improved single-aliquot regenerative-dose protocol. *Radiation Measurements*. Amsterdam. 32, p. 57-73.

RICHTER, D.; ZINK, A. J. C.; PRZEGIETKA, K. R.; CARDOSO, G. O.; GOUVEIA, M. A.; PRUDÊNCIO, M. I. (2003) - Source calibrations and blind test results from the new luminescence dating laboratory at the Instituto Tecnológico e Nuclear, Sacavém, Portugal. *Ancient TL*. Aberystywth. 21:1, p. 43-48.

SINGARAYER, J. S.; BAILEY, R. M. (2003) - Further investigations of the quartz optically stimulated luminescence components using linear modulation. *Radiation Measurements*. Amsterdam. 37, p. 451-448.

TSUKAMOTO, S.; RINK, W.J.; WATANUKI, T. (2003) - OSL of tephric loess and volcanic quartz in Japan and an alternative procedure for estimating De from a fast OSL component. *Radiation Measurements*. Amsterdam. 37, p. 459-465.

ZIMMERMAN, D.W. (1971) - Thermoluminescene dating using fine grains from pottery *Archaeometry*. Oxford. 13, p. 29-52.

ZINK, A.J.C.; QUERRE, G.; PORTO, E. (2002) - Automation of the chemical preparation for luminescence dating. *LED2002. 24-28 June 2002, Reno (Abstract*).